OMICS A Journal of Integrative Biology
Volume 14, Number 6, 2010

DOI: 10.1089/omi.2010.0031

Functional Genomics of Drug-Induced Ion Homeostasis Identifies a Novel Regulatory Crosstalk of Iron and Zinc Regulons in Yeast

Nathalie Landstetter,[1] Walter Glaser,[1] Christa Gregori,[1] Joachim Seipelt,[2] and Karl Kuchler[1]

Abstract

Pyrrolidine dithiocarbamate (PDTC), a known inhibitor of NFκB activation, has antioxidative as well as antiviral activities. PDTC is effective against several virus families, indicating that its antiviral mechanism targets host rather than viral functions. To investigate its mode of action, we used baker's yeast as a simple eukaryotic model system and two types of genome-wide analysis. First, expression profiling using whole-genome DNA microarrays identifies more than 200 genes differentially regulated upon PDTC exposure. Interestingly, the Aft1-dependent iron regulon is a main target of PDTC, indicating a lack of iron availability. Moreover, the PDTC-caused zinc influx triggers a strong regulatory effect on zinc transporters due to the cytoplasmic zinc excess. Second, phenotypic screening the EUROSCARF collection for PDTC hypersensitivity identifies numerous mutants implicated in vacuolar maintenance, acidification as well as in transport, mitochondrial organization, and translation. Notably, the screening data indicate significant overlaps of PDTC-sensitive genes and those mediating zinc tolerance. Hence, we show that PDTC induces cytoplasmic zinc excess, eliciting vacuolar detoxification, which in turn, disturbs iron homeostasis and activates the iron-dependent regulator Aft1. Our work reveals a complex crosstalk in yeast ion homeostasis and the underlying regulatory networks.

Introduction

Pyrrolidine dithiocarbamate (PDTC), a low-molecular weight thiol compound, is a multifunctional drug exerting various effects in biological systems. For instance, it is an inhibitor of the nuclear factor kappa B (NFκB) activation (Schreck et al., 1992), and it can exert both pro-apoptotic and anti-apoptotic effects depending on the cellular host system (Erl et al., 2000; Morais et al., 2006). Furthermore, PDTC shows inhibitory effects on protein degradation (Hayakawa et al., 2003; Kim et al., 2004), and elicits an oxidative stress response by inducing transcription of the manganese superoxide dismutase and the heme oxygenase HO-1 (Borrello and Demple, 1997; Hartsfield et al., 1998). Interestingly, PDTC displays antiviral activity against picornaviruses including human rhinovirus, poliovirus, and coxsackievirus (Gaudernak et al., 2002; Lanke et al., 2007), as well as on influenza viruses, the latter being orthomyxoviruses with a very different life cycle (Uchide et al., 2002). Interestingly, PDTC prevents polyprotein processing and reduces virus titers mainly by shuttling zinc ions into host cells (Krenn et al., 2005). Because different virus families are inhibited, and no resistant strains have been observed to date, it has been speculated that the antiviral mechanism of PDTC might target host cell rather than viral functions. To gain insight into the cellular mechanisms and control programs affected by PDTC, we decided to use the yeast *Saccharomyces cerevisiae* as a simple eukaryotic model system, because PDTC shows antifungal activity in yeast. Yeast is a model organism for chemogenomic approaches that has proven itself invaluable for the unraveling of many fundamental biological processes including drug target gene identification (Giaever, 2003; Parsons et al., 2004). Due to the high evolutionary conservation of many cellular processes (Foury, 1997), phenotypic screening techniques in yeast have become advantageous for drug development and pharmacokinetic studies (Bharucha and Kumar, 2007). Phenotypic screening of the haploid yeast deletion collection revealed important insights in cellular processes and pathways affected by certain stress conditions or drug treatments (Parsons et al., 2004; Tucker and Fields, 2004). Likewise, microarray profiling using whole-genome DNA microarrays can yield conclusive insights into the mode of action of a drug and the genes modulated by comparing untreated to drug exposed cells (Hughes et al., 2000). For example, microarray profiling for a set of different stresses and environmental conditions identified an extensive

[1]Medical University Vienna, Max F. Perutz Laboratories, Campus Vienna Biocenter, A-1030 Vienna, Dr. Bohr-Gasse 9/2, Austria.
[2]Medical University Vienna, Max F. Perutz Laboratories, Campus Vienna Biocenter, A-1030 Vienna, Dr. Bohr-Gasse 9/3, Austria.

transcriptional network underlying cellular stress responses (Gasch et al., 2000), but also enables the discovery of direct as well as off-targets of bioactive compounds (Ericson et al., 2008; Parsons et al., 2006).

The field of chemical genetics and chemogenomics aims at drug target identification by inhibiting gene functions in an entire organism using small-molecule exogenous xenobiotics. Lack of a gene in combination with a sublethal dose of a drug can have a synthetic lethal effect such as reduced fitness, thus enabling to identify the pathway or the drug target that mediates the toxic effect imposed by the drug (Stockwell, 2000). In this study we aimed to apply this chemical genetic approach to decipher the mode of action of PDTC, and perhaps to identify a target gene for PDTC inhibition. Thus, we performed microarray-based profiling of the yeast PDTC response, as well as a genome-wide functional screening of the EUROSCARF yeast gene deletion collection. Strikingly, our data unravel major changes in cellular ion homeostasis, including the crosstalk of iron and zinc regulatory networks.

Materials and Methods

Yeast strains and growth conditions

All yeast strains used in this study are listed in the Supplementary Table S1. Rich medium [yeast extract-peptone-dextrose (YPD)] was prepared as described in Kaiser et al. (1994). Unless otherwise indicated, all yeast strains were routinely grown at 30°C. Growth inhibition assays were performed with logarithmically grown cells, which were adjusted to an optical density at 600 nm (OD_{600}) of 0.2. Equal volumes of 1:10 serial dilutions were spotted onto agar plates containing different drug concentrations. *Schizosaccharomyces pombe* was grown on solid YES medium as described elsewhere (Moreno et al., 1991). For viability assays, cells were grown in liquid medium supplemented with PDTC and/or metal ions for 24 h. Afterward, cells were plated onto YPD plates and colony-forming units were determined after 48 h incubation. Stressed cells were normalized to untreated wild-type cells. PDTC was purchased from Alexis Biochemicals (Lausen, Switzerland).

Functional screening for sensitivity phenotypes in the presence of PDTC

For large-scale phenotypic profiling, the about 4,800 haploid viable single gene deletion strains of the EUROSCARF deletion collection (http://web.uni-frankfurt.de/fb15/mikro/euroscarf/index.html) were grown on YPD plates in a 96-well format. For transferring strains to PDTC-containing plates and control YPD plates, we used the RoToR HAD robot (Singer Ltd., Roadwater, UK). Growth was inspected after 2, 4, and 6 days incubation at 30°C. After incubation, plates were scanned with an HPScanjet G3010, using the Adobe Photoshop CS3 software. All strains displaying PDTC sensitivity in the first screening were manually respotted for confirmation. Equal volumes of serial dilutions of exponentially growing cells ranging from an OD_{600} of 0.2 to 2×10^{-4} were spotted onto PDTC plates and control plates.

Preparation of total yeast RNA and microarray analysis

Yeast cells were grown in YPD to an OD_{600} of about 0.4. The medium was supplemented with 75 μM PDTC; untreated control cells and PDTC-treated cells were harvested as 50-mL samples after 1, 3, and 5 h, washed with ice-cold water, and frozen immediately at −80°C. Total RNA was prepared by the hot phenol method (Sambrook et al., 2001). About 20 μg of total RNA from each sample were used for cDNA synthesis using 200 units of Superscript II reverse transcriptase (Invitrogen, Carlsbad, CA, USA) with either Cy3-dCTP or Cy5-dCTP. Labeled cDNAs were pooled, and RNA was hydrolyzed for 20 min in 50 mM NaOH at 65°C, followed by neutralization with acetic acid and probe cleanup with the CyScribe GFX purification kit (Amersham, Arlington Heights, IL, USA).

Hybridization to whole genome cDNA microarrays (Yeast 6.4K Arrays, Microarray Centre, University Health Network, Toronto was done in DigEasyHyb (Roche Applied Science) solution at 37°C overnight with 70 μg/mL of salmon sperm DNA as a carrier. Microarrays were washed three times in 1× SSC, 0.1% SDS at 50°C, followed by a 1-min wash in 1× SSC at room temperature. Glass slides were spun dry for 5 min at 500 rpm in a tabletop centrifuge, and scanned in an Axon 4000B scanner (Molecular Devices, Menlo Park, CA, USA). All microarray experiments were carried out with three independent RNA preparations and at least one technical replicate using dye-swaps.

Computational analysis of microarray data and screening results

Gridding and spot identification on microarrays were performed using the Gene Pix Pro4.1 software (Axon, Union City, CA, USA). For preprocessing, the background was subtracted and subsequently normalized, using the print-tip loess method of the limma Bioconductor/R package (Wettenhall and Smyth, 2004). To identify differentially expressed genes, a linear model and empirical Bayesian-moderated F-statistics were used with cutoff values of 0.001 for the adjusted p-value and a twofold expression change, as well as A-values $\geq$7 (Smyth, 2004).

Genes identified either on the microarrays or in the functional screening were grouped by gene ontology enrichment according to the predicted biological process using the Gene Ontology (GO) Termfinder program provided by the *Saccharomyces* Gene Database (www.yeastgenome.org). Clustering of differentially expressed genes was performed using the MEV software using the linkage method and Euclidean distance (Saeed et al., 2003, 2006). The clustering files are found in Supplementary Figure S1. All microarray experiments were carried out under full MIAME compliancy and data have been submitted to the *Array Express* database.

Northern blot analysis

For Northern blots, 15 μg of total RNA were fractionated in a 1.4% agarose gel and transferred to nylon membranes (Amersham Biosciences). Methylene blue staining was used as control for equal RNA loading. Northern blots were prehybridized for 3 h at 65°C. PCR-amplified probes were radiolabeled by incorporation of [α-32P]dCTP using a MegaPrime labeling kit (Amersham Biosciences). Radiolabeled probes were purified on NICK columns (Amersham Biosciences) before adding to the prehybridization solution. Membranes were washed at 65°C three times each in 2 × SSC, 1% SDS, in 1 × SSC 1% SDS and exposed to X-ray films at −80°C.

β-Galactosidase assays and immunoblotting

Cells containing a genomically integrated *FET3*–lacZ reporter construct OCY355 (Kumanovics et al., 2008) were grown in YPD medium to the mid-exponential growth phase. Cells were treated with 100 μM PDTC or left untreated. β-Galactosidase assays were performed in triplicate with cell extracts as described in Kaiser et al. (1994).

For immunoblotting, total cell-free protein extracts were prepared by the trichloroacetic acid method exactly as described previously (Mamnun et al., 2004). Cells were grown to the mid-logarithmic growth phase, left untreated or stressed with 100 μM PDTC for 2 h. Cell lysates equivalent to 0.5 OD_{600} units were resolved by 7.5% SDS-PAGE and transferred to nitrocellulose membranes. Polyclonal α-Swi6 antibodies (kindly provided by Kim Nasmyth) were used to verify equal loading.

Fluorescent detection of zinc influx into yeast cells

About 2×10^8 cells of a *pdr5*Δ *pdr12*Δ double deletion strain (kindly provided by Ralf Egner) were loaded with 30 μM mag-fura-2 (Molecular Probes, Invitrogen) for 30 min in 1× TBS; cells were washed three times and finally resuspended in 10 mL TBS. Experiments were performed in 3-mL silica cuvettes containing 2-mL aliquots of a cell suspension with constant agitation. Intracellular zinc accumulation was monitored with real-time kinetics over a 500-s period using a spectrofluorimeter LS-55 (Perkin-Elmer, Norwalk, CT, USA) by continually alternating the excitation wavelengths of 340 and 380 nm in 20-ms intervals and recording the emission at 509 nm; 10 μM $ZnSO_4$, 10 μM $CaCl_2$, or 10 μM $CuSO_4$, and 100 μM PDTC and 50 μM EDTA were added to the cell suspension at indicated time points.

Results

PDTC shows antifungal activity in various yeast species

The effect of PDTC on growth of *Saccharomyces cerevisiae*, *Candida albicans*, *Candida glabrata,* and *Schizosaccharomyces pombe* was analyzed by growth inhibition assays on agar plates. Serial dilutions of the yeast cells were spotted onto PDTC supplemented plates. Cell growth was inhibited in both nonpathogenic yeasts as well as in *Candida* spp, although not to the same extent (Fig. 1A). Namely, *S. cerevisiae*, *C. albicans,* and *S. pombe* were sensitive at 30 μM PDTC, whereas *C. glabrata* was more resistant growing up to a concentration of 75 μM PDTC. However, it is known that *C. glabrata* shows increased inherent tolerance to antifungals such as azoles when compared to *S. cerevisiae* and *C. albicans* (Pfaller and Diekema, 2004).

Moreover, we performed growth curves with *Saccharomyces cerevisiae* wild-type cells to investigate PDTC tolerance in liquid culture. Cells were grown in rich medium supplemented with increasing concentrations of PDTC and OD_{600} was monitored over time. The growth curves showed a dose-dependent growth inhibition (Fig. 1B). At low concentrations (25 μM), PDTC treated cells responded with an elongated lag-phase and a delayed period to reach the stationary phase. At higher concentrations (150 μM), PDTC caused fungistatic growth inhibition. This broad antifungal activity of PDTC suggested using yeast as a model system by exploiting well-established large-scale screening techniques for PDTC drug target identification.

The PDTC transcriptome comprises of more than 200 genes

To identify regulatory effects and the kinetics of PDTC action on the yeast transcriptome, we performed whole-genome DNA microarray experiments. Therefore, wild-type yeast cells were grown to the mid-logarithmic growth phase in rich medium, and treated with PDTC for 1, 3, or 5 hours (Fig. 1B). Transcript data of three independent biological and one technical replicate at every time point were generated, and PDTC-treated versus untreated cells were compared. Microarray results were statistically evaluated considering changes more than twofold as significant. All major changes were confirmed at RNA level by Northern analysis.

PDTC-induced changes in transcriptome profiles consisted of more than 200 differentially expressed genes (Table 1), indicating a major transcriptional shift in yeast. GO enrichment of the microarray data using the *Saccharomyces* Gene Database GO Termfinder revealed that the main functional categories included the iron regulon, aerobic respiration, and general metabolic changes. To identify the regulatory associations of the differentially expressed genes, we clustered the genes with YEASTRACT (Teixeira et al., 2006) (see Supplementary Table S2). Thereby, differentially expressed genes identified through microarrays were grouped according to their transcription factors or potential regulators. Supporting the findings of the GO enrichment, the main transcription factors required for general and oxidative stress response genes, as well as proteasome and multidrug resistance genes were found. These included the transcriptional regulators Yap1, Msn2/4, Rpn4, and Sfp1 correlating with the activation of general stress response genes as well as with repression of ribosomal genes under various stress conditions (Gasch et al., 2000; Wu et al., 2008). Interestingly, the clustering specifically identified the iron-responsive transcription factor Aft1 as one of the major responders.

PDTC activates the Aft1-dependent iron regulon in yeast

Among the highest induced genes, we identified several genes of the high-affinity iron uptake system (*FET3*, *ARN4*), as well as cell wall mannoproteins required for siderophore-bound iron retention (*FIT1*, *FIT2*, *FIT3*). This set of genes is referred to as the yeast iron regulon, which is under the control of the transcription factors Aft1/Aft2. The iron regulon is rapidly activated under iron-limiting conditions (Yamaguchi-Iwai et al., 1995, Yun et al., 2000). Upon iron depletion, Aft1 traffics into the nucleus to orchestrate an immense cellular cascade response, inducing first the iron uptake machinery and mobilization of intracellular iron from storage compartments, followed by adaptations of metabolic iron usage (Yamaguchi-Iwai et al., 2002). This includes a switch to less iron-consuming pathways, shutting down nonessential pathways while preserving essential ones (Kaplan and Kaplan, 2009). The pathways regulated in response to iron changes include the biotin, glutamate, and purine biosynthetic pathways, as well as the TCA cycle. Furthermore, genes involved in heme biosynthesis and in the respiratory chain are

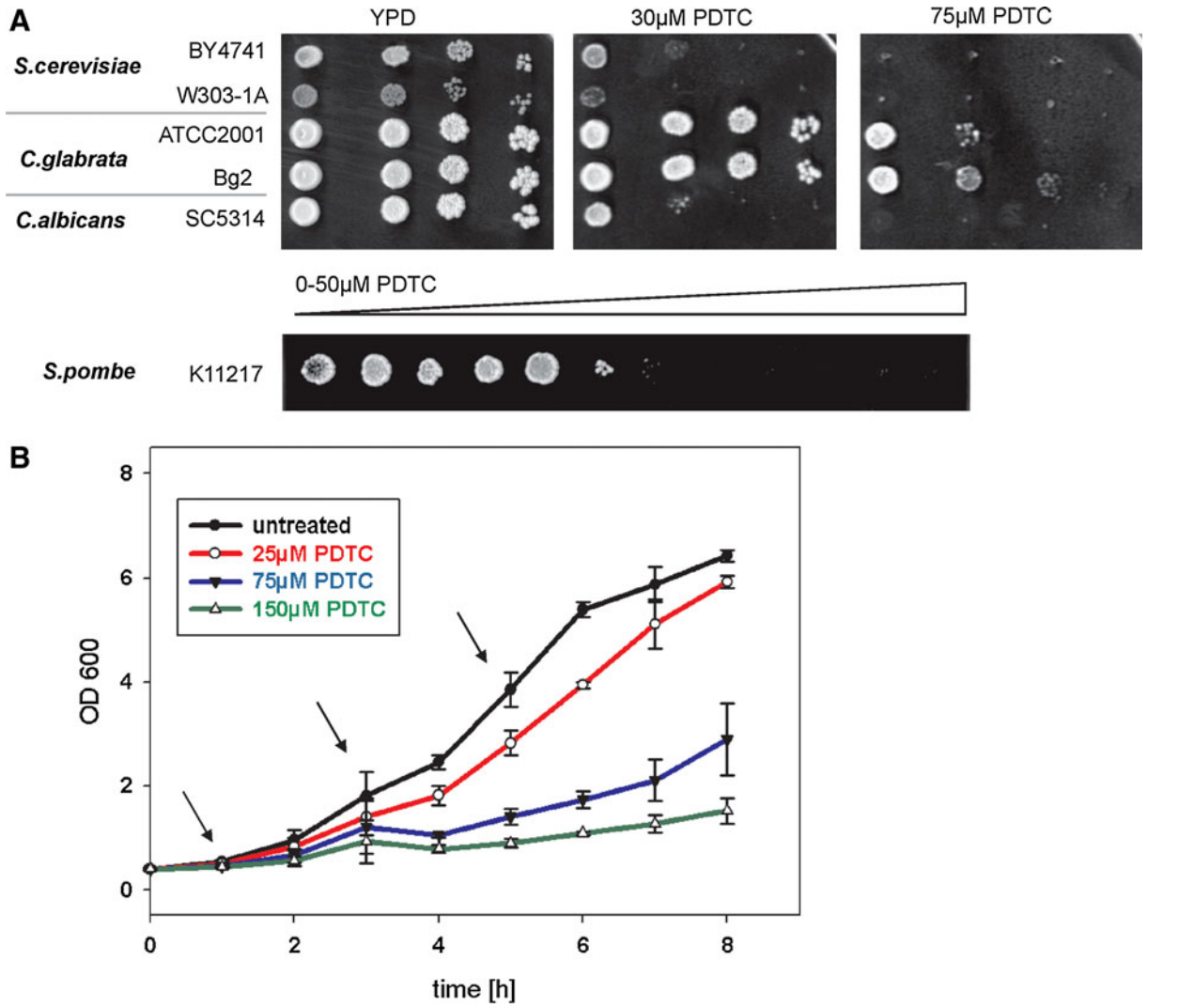

FIG. 1. PDTC inhibits growth of several yeast species. (**A**) The effect of PDTC on growth of various yeast species was examined by spot assays on solid medium. Logarithmically growing wild-type strains were spotted in serial dilutions ranging from OD_{600} of 0.2 to 2×10^{-4} onto YPD and PDTC-containing plates and grown at 30°C for 2 days. *S. pombe* (OD_{600} of 0.2) was spotted on YES medium containing a gradient from 0 to 50 μM PDTC. (**B**) Growth curves of the *S. cerevisiae* wild-type strain BY4741 with increasing concentrations of PDTC. Cells were grown in rich medium supplemented with PDTC for 8 h at 30°C. Growth was monitored by measuring OD_{600} every hour. Data are displayed as mean ± 1 SD of three independent growth experiments. Arrows indicate the time points at which samples were harvested for microarray analysis of unstressed cells and cells treated with 75 μM PDTC.

downregulated (Hausmann et al, 2008). Indeed, PDTC triggered both the primary and secondary wave response genes involved in iron-dependent cellular remodeling (Table 1).

To confirm the induction of the iron regulon in response to PDTC, and to investigate whether this activation is Aft1-dependent and iron-specific, we performed Northern analysis and growth inhibition assays comparing the wild-type with the *aft1*Δ strain. Activation of the iron regulon (*FIT3*, *FIT2*) in response to PDTC was fully Aft1-dependent, whereas *GRE2*, encoding a metalloreductase involved in the high osmolarity glycerol pathway, served as control for Aft1-independent induction (Fig. 2A). Furthermore, PDTC strongly induced the promoter of *FET3* encoding the ferroxidase of the high-affinity iron transport system as shown by a *FET3–lacZ* reporter assay (Fig. 2B).

Aft1 is required for growth under iron-limited conditions (Yamaguchi-Iwai et al., 1995). Consistently, the *aft1*Δ strain was hypersensitive to PDTC when compared to its corresponding wild type, suggesting that Aft1 is required for PDTC tolerance (Fig. 2C). Iron-supplementation specifically rescued this sensitivity phenotype (Fig. 2C), thus showing that PDTC must mimic or cause a lack of iron availability. Other ions such as Mg^{2+}, Ca^{2+}, Zn^{2+}, and Mn^{2+} failed to rescue the PDTC-dependent growth inhibition, and Cd^{2+} supplementation even further increased PDTC sensitivity. Notably, copper supplementation rescued growth of the *aft1*Δ strain in the presence of PDTC, but impaired PDTC tolerance of the wild-type strain. All in all, these data show that activation of the iron regulon by PDTC is Aft1-dependent and is required for PDTC tolerance.

Table 1. Functional Categories of Genes Regulated upon PDTC Stress

Categories	*Gene names*	*No. of genes*
Iron regulon Aft1/Aft2 target genes	*FTH1, SIT1, FTR1, ARN1, ARN2, CTR2, FRE1, CCS1, FET3, ENB1, FIT1, FIT2, FIT3, YLR126C, ISU2, ISU1, FTR1*	17
Carboxylic acid metabolic process	*CYS3, GCV3, SHM1, CHA1, SFA1, GLT1, GCV1, ARO3, HOM3, MET6, LPD1, ARO9, POT1, ELO1, FBA1, FAS1, ILV5, ILV2, GCV2, LEU4, LYS9, LEU9, HIS3, GDH1, CAR1, GLN1, SHM2, URA1, GTT1, URA4*	30
Purine biosynthetic process	*ADE1, ADE8, ADE5,7, ADE13, ADE17, ADE3, ADE12*	7
Stress response to drug/toxin	*AAD3, RPN4, UBC5, YCF1, SNF1, AAD6, AAD16,* YML131W, *DDR48, HOR7, LAP3, GRE2, TIR2, OYE3, HSP31, SFP1, OYE2*	17
Response to oxidative stress	YDL124W, *CTA1, TRR1, YPR1, GRX2, TRX2, STB5, SOD1, CCP1, TRX1, AHP1, ZWF1, ATX1, GLR1, PEP4*	15
Respiration and citric acid cycle	*COX6, COX5A, COX9, COX13, IDH1, ACO1, RIB3, POR1, QCR7*	9
Transport	*STP22, TRS23, INH1, VHT1, TOM6, HNM1, MUP1, TPO1, DIC1, SFH5, HXT10, HXT4, HXT5, HXT8, GAL2, HXT11, HXT12*	18
Heme and ergosterol biosynthesis	*ERG3, ERG1, ERG27, ERG11, HEM13, YHB1, YCP4*	7
Telomere maintenance	YGL039W, *NMD2, CST6, HCR1, LST7, SWD1, PNC1*	7
Transcription/ translation	*MRP8, EFB1, GCD2, RLI1, GAT1, ERB1, UTP23, SSZ1, RLP7, TUF1*	10
DNA replication/ repair	*RNR2, RNR4, DON1, WTM1, YPL033C, NNF1, RFA2, SIM1*	8
Oxidoreductase activity	*ADH7,* YDR541C, *DLD3, YGL157W, ADH6,* YNL134C	6
Other	*PHO5, PHO11, PHO86, IRC7, IZH1, FRM2, MFA1, EMI2, AGA2, KOG1, BAR1, BNR1, MSG5, LAP4, AIM46, RIB4, SLA1, EHD3, FLO9, NDE1, SNC2, PAC11, TEC1, PEX5, UGP1, RMD6, AIM18, PMI40, SCW4, CWP1, SRP40, EMI1, VHS1, YRO2, PRE8, MRH1, APT2, TIP1, LRG1, CNS1, WWM1, RPN6, DPH5, FRQ1, FMP43*	45
Unknown	YAL065C, YMR173W-A, YCR102C, YJL217W, YER156C, YGR146C, YDR476C, YOR285W, YKL088W, YDR154C, YKL030W, YPL067C, YKL066W, YLL044W, YDR271C, YBR053C, YJL068C, YFR024C, YHR213W, YAR073W, YKL171W, YEL033W, YDR119W, YLR460C, YNL208W, YCR074C	26

Wild-type yeast cells were grown to the logarithmic growth phase in rich medium, treated with PDTC for 1, 3, or 5 h. RNA was extracted and labeled samples were used to probe yeast DNA microarrays. We carried out three independent comparisons of PDTC-treated versus untreated cells considering changes more than twofold as significant. The PDTC transcriptome comprises of a general and a specific stress response, all together involving more than 200 genes that were categorized by Gene Ontology enrichment. Overlapping processes were manually collapsed. All genes affected by PDTC treatment are listed in Supplementary Table S2, including data of all time points, fold expression, and values.

PDTC treatment causes intracellular zinc overload

On the one hand, PDTC caused activation of the iron uptake machinery. On the other hand, it was striking to note that PDTC strongly altered expression of plasma membrane and vacuolar zinc transporters (Fig. 3A). In detail, expression of the plasma membrane low-affinity zinc transporter Zrt2 and the vacuolar zinc exporter Zrt3 was strongly decreased upon PDTC treatment, whereas the transporter importing zinc into the vacuole, Cot1, was highly induced. Transcript levels of the high-affinity zinc transporter Zrt1 stayed unchanged; however, Zrt1 is regulated posttranslationally via ubiquitination and endocytosis (Gitan and Eide, 2000). Although yeast lacks a cellular zinc exporter, free zinc concentrations are kept low because excess zinc is highly toxic for cells. Spare zinc is bound to proteins or stored in vesicular compartments such as the vacuole as major site of storage and detoxification (Eide, 2009).

Consistent with our notion of PDTC-induced cellular zinc excess, transcript levels of the major zinc-conserving proteins like alcohol dehydrogenases (ADHs) and superoxide dismutase 1 (Sod1) were increased on our microarrays. We confirmed induction of the cytoplasmic superoxide dismutase *SOD1* gene by Northern blotting (Fig. 3B). In the *aft1*Δ strain, *SOD1* gene induction was even more pronounced than in the wild type. Consistently, Sod1 deficiency led to increased PDTC and zinc-sensitivity, whereas deletion of the manganese superoxide dismutase Sod2 had less severe effects. (Fig. 3B and C). Interestingly, iron supplementation failed to rescue the PDTC-induced growth defect of the *sod1*Δ strain. However, this failure might be due to a previously reported increase in iron demand of the *sod1*Δ mutant per se, and its involvement in zinc detoxification (De Freitas et al., 2000; Tarhan et al., 2007). In this case, PDTC would worsen the lack of iron availability, thereby increasing the sensitivity of the *sod1*Δ strain.

To directly monitor PDTC-induced zinc accumulation inside yeast cells in real time, we used the fluorescent dye mag-fura-2. As the dye is normally effluxed from cells, all experiments were carried out in a strain lacking the ABC transporters Pdr5 and Pdr12. The excitation wavelength of mag-fura-2 is shifted from 380 to 340 nm when binding bivalent cations (Raju et al., 1989; Simons, 1993). After loading yeast cells with mag-fura-2, cells were extensively washed and $ZnSO_4$, $CuSO_4$, $CaCl_2$, or $MgCl_2$, PDTC and EDTA were added at indicated time points. Although adding $ZnSO_4$ had only minor effects on the fluorescent ratio, the supplementation of PDTC caused a rapidly increasing signal as a readout for intracellular zinc accumulation. As expected, adding EDTA reduced the signal immediately. Other metal ions including Mg^{2+}, Cu^{2+}, and Ca^{2+} had no effect on the fluorescent signal. Thus, PDTC caused an immediate influx of

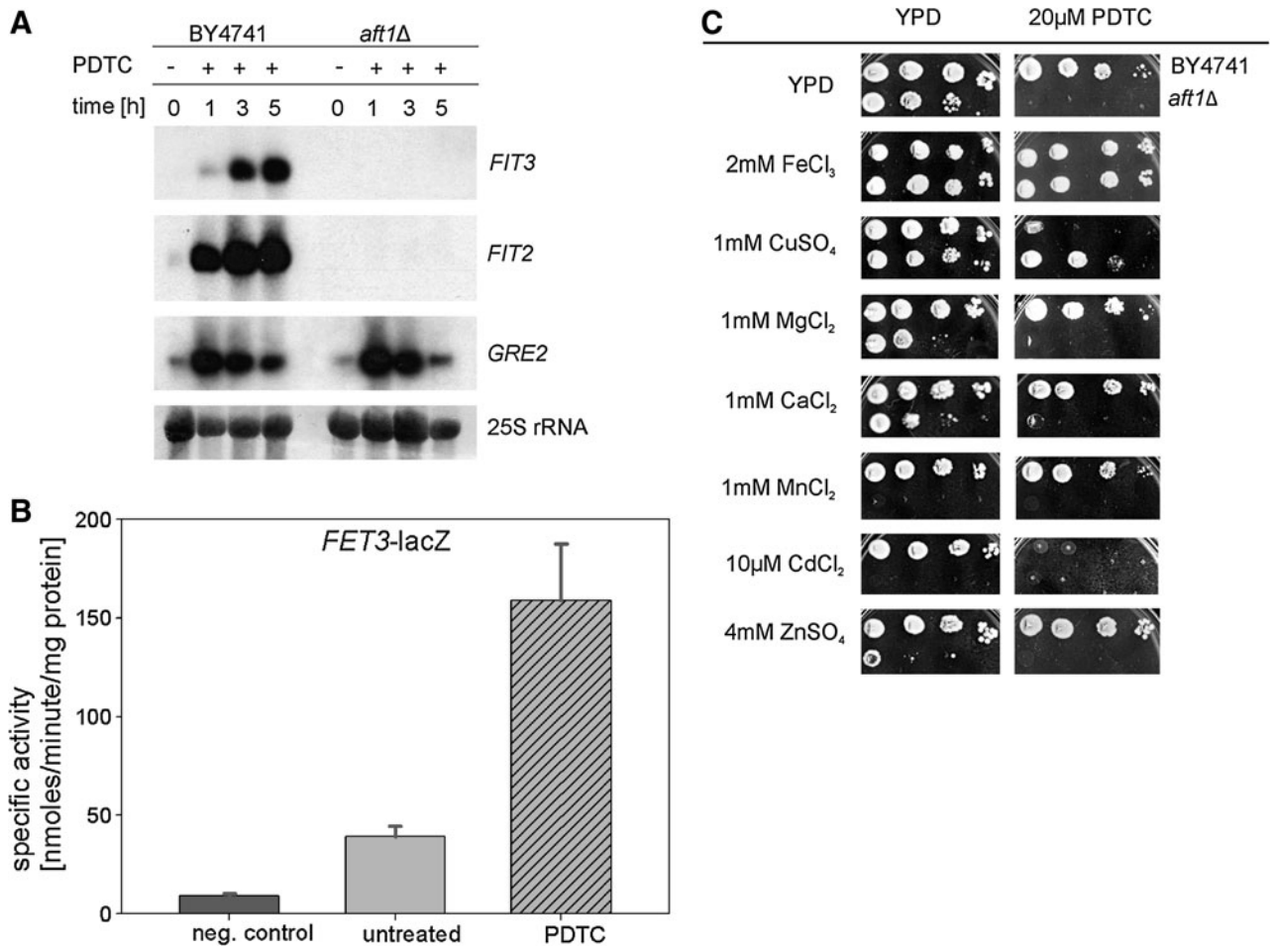

FIG. 2. PDTC activates the Aft1-dependent iron regulon. (**A**) Induction of the iron regulon is Aft1-dependent. Northern blot analysis comparing PDTC-induced gene expression of the iron-responsive genes *FIT2*, *FIT3*, and the Aft1-independent gene *GRE2* in wild-type and *aft1*Δ cells. Cells were treated for 1, 3, and 5 h with PDTC. Untreated and PDTC treated cells were harvested, total RNA was isolated for Northern blot analysis. (**B**) PDTC activates the *FET3*-promoter. Cells containing an integrated *lacZ–FET3* reporter construct were grown to the mid-log phase (OD_{600} ~0.6) in YPD and treated with 100 μM PDTC for 3 h. Cells were harvested and assayed for β-galactosidase activity. Data of a representative experiment are shown and the error bars represent ±1 SD of three replicates. (**C**) PDTC-induced growth deficiency is rescued by iron supplementation. Wild-type and *aft1*Δ cells were spotted in serial dilutions on rich media containing PDTC and/or different ions. Growth was monitored after 2 days incubation at 30°C.

Zn^{2+} ions into the yeast cells and elevated intracellular zinc levels (Fig. 4). Taken together, the observed regulation of the zinc homeostasis in response to PDTC indicates excess cytoplasmic zinc, leading to subsequent zinc detoxification by sequestration into the vacuole and by induction of zinc-binding proteins (Fig. 3A, B).

PDTC enhances a crosstalk between iron and zinc homeostasis

Because both zinc homeostasis and the iron regulon were strongly affected by PDTC, we aimed to investigate a potential underlying regulatory crosstalk between these two pathways. Supporting this notion, it was previously reported that zinc overload activates the iron regulon (Pagani et al., 2007). In addition, *aft1*Δ cells are sensitive to high concentrations of extracellular zinc, which indicates that Aft1 is required to counteract the growth defect caused by excess zinc (Pagani et al., 2007). Hence, we performed viability assays with wild-type and *aft1*Δ strains in the presence of PDTC, Zn^{2+} and Fe^{3+}, respectively (Fig. 3D). Colony-forming units were determined after 24-h stress treatment with 200 μM PDTC in liquid medium and set relative to the untreated wild type. As expected, iron supplementation rescued the cytotoxic effect of PDTC in wild-type and *aft1*Δ cells. In contrast, this effect was enhanced by excess zinc. Growth deficiency of *aft1*Δ cells on high excess zinc was rescued by iron supplementation. Strikingly, the combined effect of PDTC, iron and zinc was almost fully rescued in the *aft1*Δ background but not in the wild-type strain (Fig. 3D). These data suggest that in wild-type cells, Aft1 also controls a yet unidentified cellular function counteracting zinc detoxification, at least in the presence of PDTC.

Functional screening identifies essential processes mediating PDTC tolerance

To identify genes that confer tolerance to PDTC, we functionally screened the EUROSCARF deletion collection for

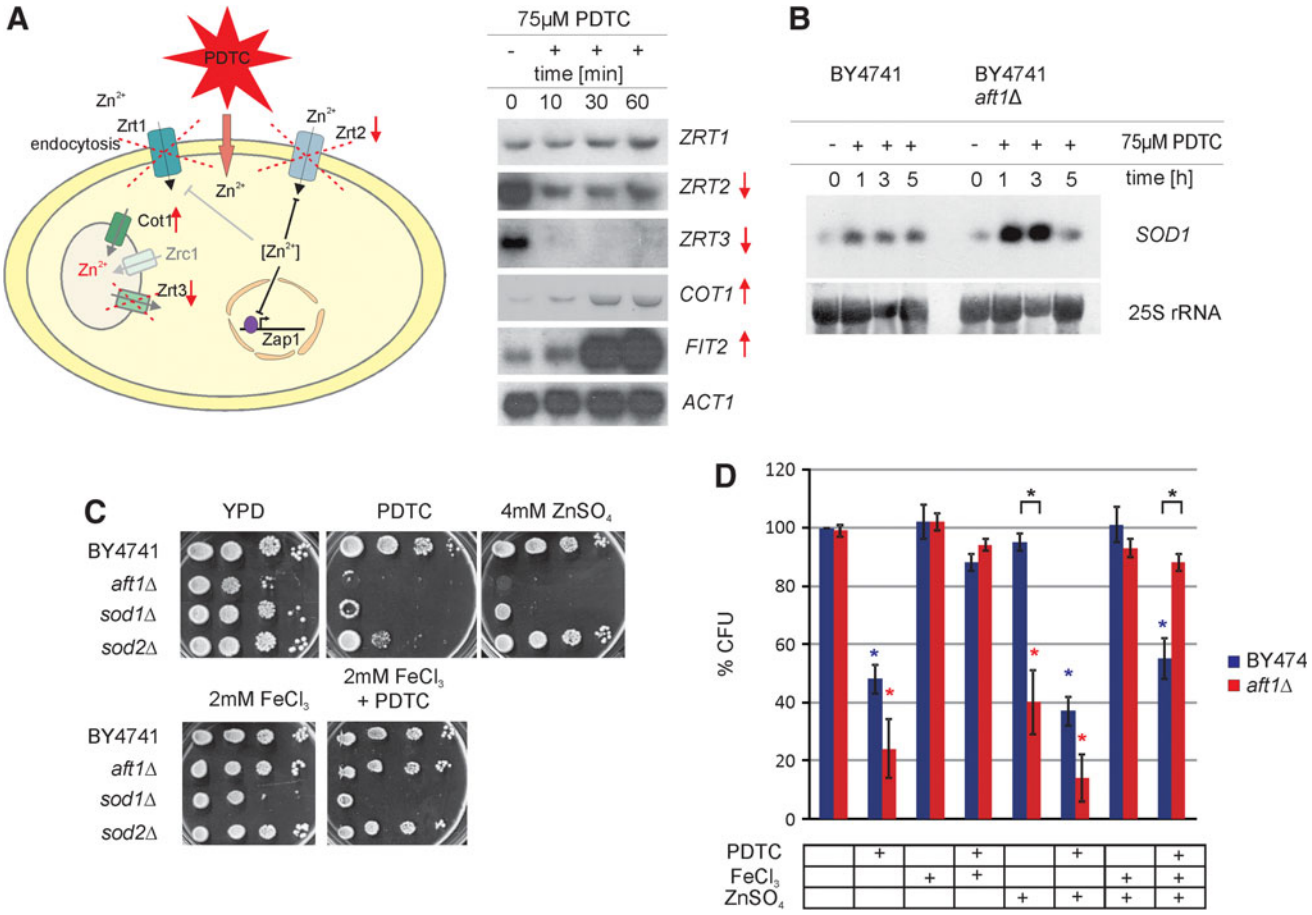

FIG. 3. PDTC causes intracellular zinc overload. (**A**) Northern blot comparing the PDTC-induced changes of transcript levels of various zinc transporters whose cellular location is indicated in the scheme on the left. These alterations in gene expression indicate intracellular zinc accumulation and subsequent vacuolar zinc sequestration. Cells were grown in rich medium to an OD_{600} ~0.5, 75 μM PDTC was supplemented and cells were harvested at the indicated time points and prepared for Northern analysis. (**B**) PDTC induces the transcript levels of the copper/zinc superoxide dismutase *SOD1* gene. Cells were treated with PDTC, harvested at the indicated time points, and total RNA was prepared for Northern analysis. (**C**) Deletion of the *SOD1* gene renders cells zinc and PDTC-hypersensitive. Wild-type and deletion mutants were spotted in serial dilutions (OD_{600} of 0.2 to 2×10^{-4}) on YPD plates supplemented with 20 μM PDTC, 4 mM $ZnSO_4$ and 2 mM $FeCl_3$, respectively. Growth was monitored after a 2-day incubation at 30°C. (**D**) Cell viability assays to investigate the nature of a probable crosstalk between iron and zinc homeostasis. Wild-type and *aft1*Δ were grown in liquid rich medium for 24 h in the presence of PDTC, $ZnSO_4$, and $FeCl_3$, respectively. Afterward, cells were plated on YPD and colony forming units (CFU) were determined after a 2-day incubation at 30°C. Data are presented as percent CFU relative to the untreated wild-type. Error bars represent ± 1 SD of three independent growth experiments; stars indicate significance of data valued by a Students *t*-test.

altered growth in the presence of PDTC. Therefore, strains of the collection were replicated on YPD and PDTC-containing plates and grown at 30°C for 6 days monitoring growth every day. The previously identified PDTC hypersensitivity of the *aft1*Δ strain was used as a control in the screening procedure. Among more than 4,800 haploid single deletion strains, we identified some 140 mutants as PDTC hypersensitive (see Supplementary Table S2). Mutants showing increased PDTC sensitivity were manually respotted in serial dilutions on several PDTC concentrations to reconfirm the phenotype. To categorize the PDTC-sensitive strains, we grouped them based on GO enrichment using the *Saccharomyces* Gene Database GO Termfinder (Fig. 5A). The main functional categories comprised of vacuolar acidification and vacuolar transport, protein modifications, mitochondrial organization, and translation. Interestingly, many mutants related to membrane and vesicular transport or trafficking systems were PDTC sensitive [e.g., endosomal sorting complex required for transport (ESCRT); Golgi-associated retrograde protein complex (GARP), HOPS complex].

Furthermore, mutants disrupting vacuolar trafficking including vacuolar protein sorting genes such as *VPS3*, *VPS4*, *VPS8*, *VPS18*, *VPS33*, *VPS41*, *VPS45*, as well as function and assembly of the V-ATPase such as *VMA8*, *VMA22*, *VMA2*, *TFP1*, *VMA21*, *VMA6*, and *PPA1* were PDTC sensitive, suggesting that vacuolar biogenesis and maintenance is pivotal for cells responding to PDTC.

The vacuole is the main storage and detoxification compartment in yeast. Thus, components involved in vacuolar biogenesis and trafficking are essential under various stress

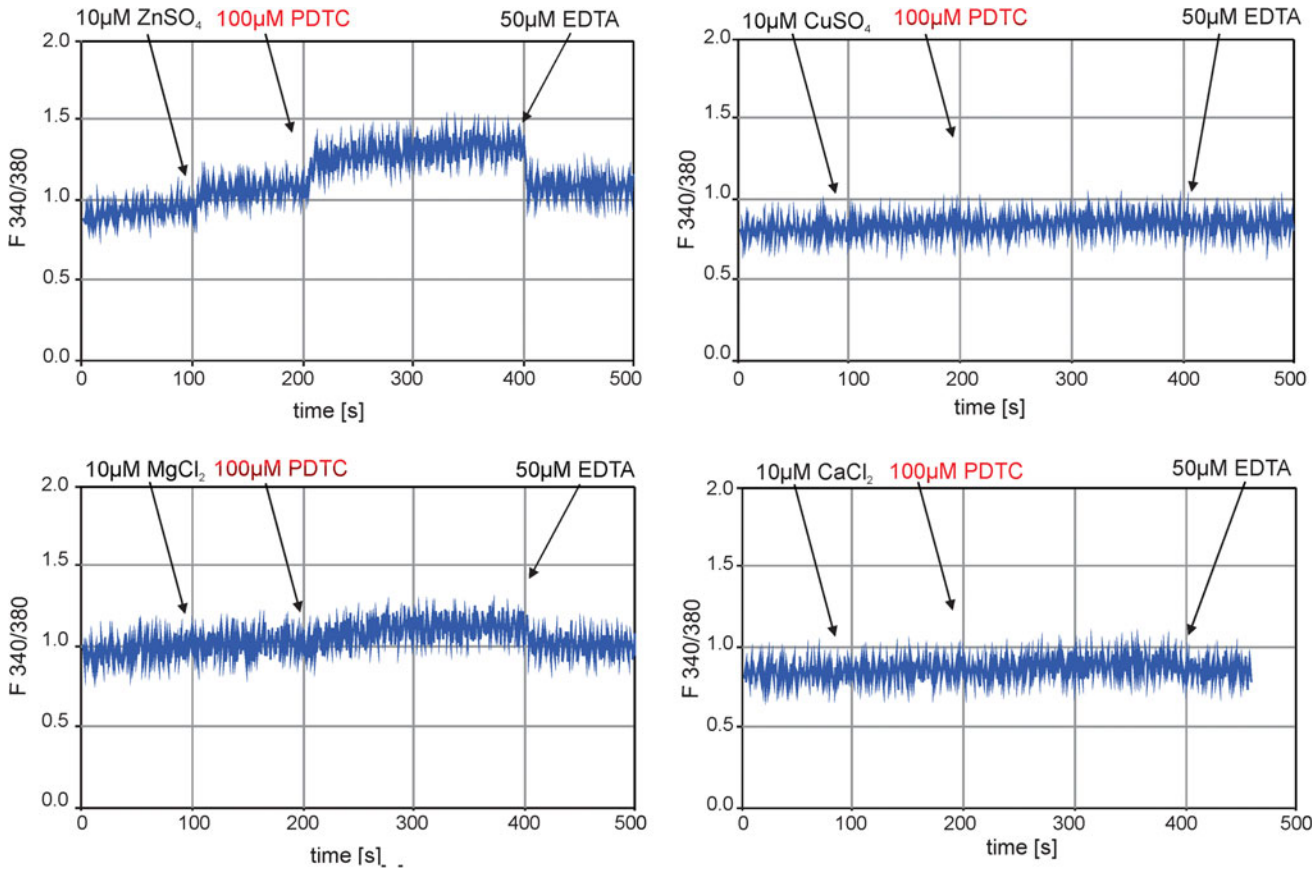

FIG. 4. PDTC induces immediate influx of zinc ions into yeast cells. Cells were loaded with the mag-fura-2 dye and fluorescence was monitored in real time after adding metal ions such as $ZnSO_4$, $CaCl_2$, $CuSO_4$, $MgCl_2$, PDTC, and EDTA at the indicated time points. The excitation wavelength of mag-fura-2 is shifted by binding bivalent metal ions. Thus, change of the fluorescent ratio of F340/380 nm following addition of zinc and PDTC, but not by calcium, magnesium, or copper, show accumulation of intracellular labile zinc.

conditions. Remarkably, we found a significant overlap of PDTC-sensitive mutants (Fig. 5B) and deletion strains sensitive to excess zinc, cadmium, oxidative stress, and alkaline pH (Jin et al., 2008; Outten et al., 2005; Pagani et al., 2007; Serrano et al., 2004). For example, a functional V-ATPase is crucial for establishing a proton gradient across the membrane to ensure vacuolar import of ions, especially for zinc sequestration (MacDiarmid et al., 2002). Thus, PDTC tolerance requires several cellular mechanisms and processes to avoid a collapse of cellular ion homeostasis.

Discussion

In this study, we exploit yeast and a chemical–genetic approach combining transcriptional profiling and phenotypic screening techniques to identify possible cellular targets of the antiviral drug pyrrolidine dithiocarbamate (PDTC). The transcriptional profiling indicates that PDTC massively disturbs metal ion homeostasis, including a strong induction of the iron regulon, as well as regulation of zinc transport. The screening of the yeast gene deletion collection for mutants with increased PDTC susceptibility identifies numerous genes essential for the PDTC response, including those required for vacuolar functions and transport complexes.

The transcriptional changes upon PDTC treatment involve more than 200 genes, including general stress response genes. Strikingly, we detect a specific activation of the Aft1 transcription factor driving the iron regulon. Beside iron deprivation, the iron regulon is activated by various stress conditions, ranging from changes in ion concentrations such as excess zinc (Pagani et al., 2007) or cobalt (Stadler and Schweyen, 2002) to physiological changes induced by lactic or acetic acid (Kawahata et al., 2006), as well as glucose depletion occurring during the diauxic shift (Haurie et al., 2003). Moreover, drugs such as the fungicide mancozeb (Santos et al., 2009), chloroquine toxicity (Emerson et al., 2002), hydroxyurea (Dubacq et al., 2006), or the anticancer drug cisplatin (Kimura et al., 2007) mimic iron depletion and thus trigger activation of the iron regulon.

Like PDTC, the fungicide mancozeb is a dithiocarbamate that complexes manganese and zinc and also activates the Aft1 transcription factor (Santos et al., 2009). Proteomic analysis suggests that mancozeb induces oxidative stress response genes, genes involved in translation, and protein degradation (Santos et al., 2009). An important property of dithiocarbamates is their metal chelating activity, thereby forming lipophilic dithiocarbamate–metal complexes and facilitating metal entry into cells (Krenn et al., 2005). Mag-fura-2 experiments show an immediate PDTC-caused influx of Zn^{2+}

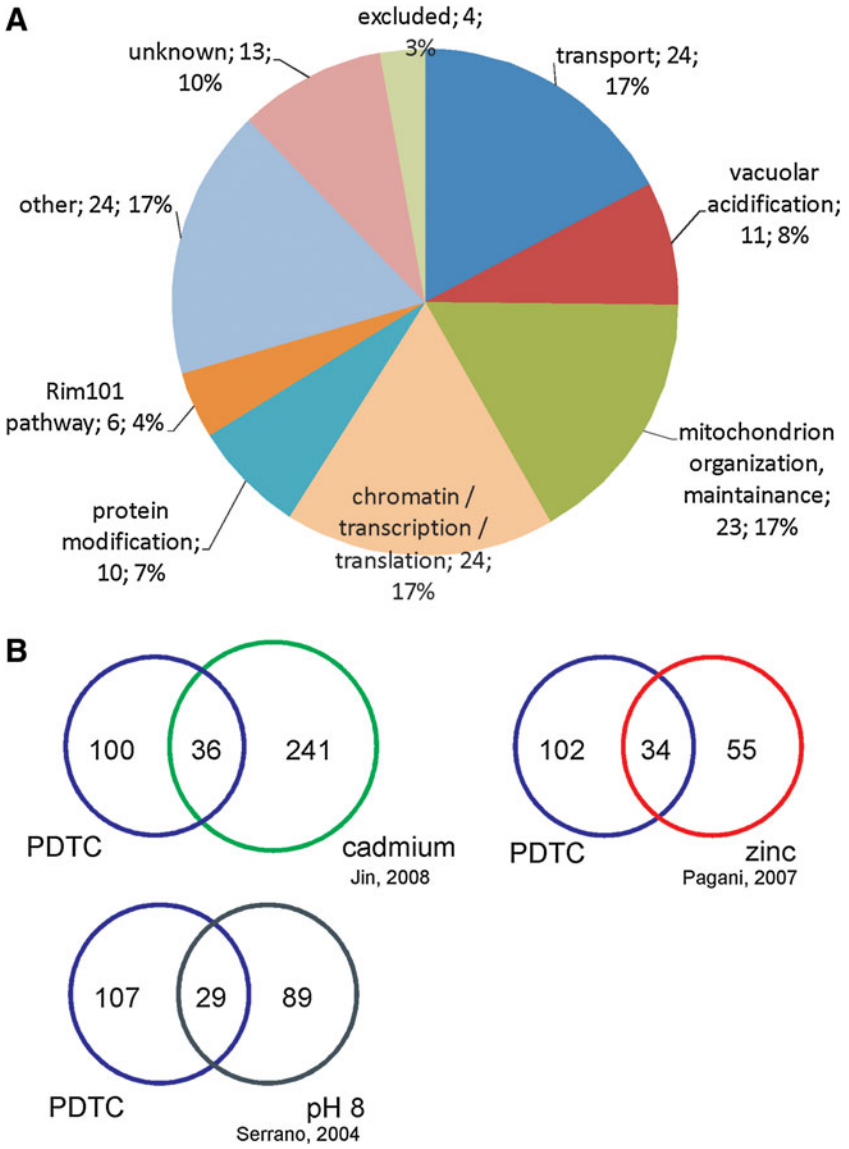

FIG. 5. Functional screening identifies processes mediating PDTC tolerance. (**A**) Functional categories of genes required for PDTC tolerance in yeast. The about 4,800 deletion strains were screened on YPD and PDTC-containing plates using a Singer RoToR HAD Robot. Growth was monitored after 2 days. Sensitive strains were verified by manual respotting and clustered into functional categories using the Gene Ontology termfinder. The number of genes per category and the percentages of each category to the dataset are indicated. All PDTC-sensitive genes are listed in Supplementary Table S2. (**B**) Venn diagrams showing the overlap of PDTC-sensitive genes and genes required during zinc and cadmium toxicity, as well as under alkaline pH conditions. Screening data for comparison were taken from published datasets (Jin et al., 2008; Pagani et al., 2007; Serrano et al., 2004).

ions into yeast cells. Thus, by changing the delicate ion balance inside cells, excess ions alter enzyme activities and metabolic functions. Thus, PDTC and dithiocarbamates in general might mask significant amounts of intracellular iron or disturb the intracellular zinc/copper homeostasis to drive induction of the iron regulon.

Maintenance of a proper metal ion homeostasis is of pivotal importance for yeast viability and metabolic functions. Crosstalk between responses to different ions has been proposed due to overlapping regulatory networks. For instance, iron and copper are tightly connected, because copper is the essential cofactor in the high-affinity iron permease complex Ftr1/Fet3 (Gross et al., 2000). Consequently, inhibition of copper uptake results in reduced iron uptake. Fet3 is a multicopper ferroxidase whose deletion renders cells highly sensitive to transition metal stress, alkaline pH, and causes impaired growth on ethanol and galactose/raffinose (Rutherford and Bird, 2004). Moreover, relationships between cobalt–iron (Stadler and Schweyen, 2002) and zinc–iron (Pagani et al., 2007; Santos et al., 2003) responses are known. Notably, the vacuolar transporter Cot1 normally involved in zinc transport into the vacuole and cobalt accumulation, is induced under iron-limited conditions (Li and Kaplan, 1998). High excess of zinc disrupts iron homeostasis by altering the intracellular iron content and iron-dependent respiratory enzyme activities such as cytochrome *c* oxidase, and aconitase,

connecting zinc, iron, and iron/sulfur cluster (ISC) metabolism (Pagani et al., 2007; Santos et al., 2003). Studies of the yeast *ionome*, as well as the interplay of alkaline pH stress and ion metabolism confirm a tight and dynamic coregulation at genomic (Eide et al., 2005; Serrano et al., 2002, 2004) and perhaps at proteomic and regulatory levels.

We here show the impact of various metal ions in combination with PDTC on ion homeostasis (Fig. 2C). For example, the *aft1*Δ strain is sensitive to nickel, calcium, manganese, cobalt, zinc, as well as alkaline pH (Serrano et al., 2004; Stadler and Schweyen, 2002). These growth phenotypes can be compensated by the supplementation of high iron to the growth media, thereby increasing cellular iron concentrations. In the case of glucose exhaustion, addition of iron fails to rescue the growth defect, indicating two independent signals inducing the iron regulon (Haurie et al., 2003). In cells lacking the *AFT1* gene, the copper-binding metallothionein Cup1 is highly induced upon PDTC treatment, which might explain the increased copper-tolerance compared to the wild type (data not shown). Consistent with the fact that PDTC acts as a zinc ionophore mediating zinc influx into HeLa cells (Krenn et al., 2005) as well as yeast cells (Fig. 4), it triggers changes in transcript levels of certain zinc transporters due to the intracellular ionic imbalance.

By functionally screening the yeast gene deletion collection for PDTC-sensitive strains, we identify genes involved in vacuolar functions and transport complexes (Fig. 5A) that are also essential under excess zinc conditions (Fig. 5B) (Jin et al., 2008; Pagani et al., 2007). For example, a functional V-ATPase is required for establishing a proton gradient across the vacuolar membrane and for zinc storage. Indeed, mutants lacking a functional V-ATPase are both zinc- and PDTC-hypersensitive. Furthermore, the chemical–genomic profile of yeast cells demonstrates that mutants involved in endosome transport, transcription, vacuolar degradation, and function of the V-ATPase are sensitive to multiple stress conditions (Hillenmeyer et al., 2008).

Taken together, and based on our data, we propose the "ionic imbalance" model for the cellular response to PDTC exposure and the PDTC mechanism of action (Fig. 6). Zinc excess as caused by PDTC (Fig. 3A) triggers dynamic expression changes of zinc transporter genes and activation of the iron regulon, whose main transcriptional activator Aft1 is required to counteract ion toxicity as well as alkaline pH stress (Pagani et al., 2007; Serrano et al., 2004; Stadler and Schweyen, 2002), thus orchestrating the adaptive regulation of ion homeostasis pathways. This rapid response regulation prevents further zinc uptake, followed by subsequent activation of the Aft1 regulon. Viability assays investigating the supplementary effect of zinc and iron on PDTC-treated cells point toward crossregulatory networks, linking zinc and iron homeostasis (Fig. 3D). Iron supplementation rescues the PDTC-induced growth defects in both wild-type and *aft1*Δ cells. By contrast, and as expected, additional zinc influx in combination with PDTC is highly toxic (Fig. 3D). By investigating cumulative or additive effects of zinc plus iron in combination with PDTC treatment, the *aft1*Δ mutant survives, whereas the wild type is hypersensitive. This suggests that Aft1 in wild-type cells also controls a yet unidentified cellular function, which counteracts zinc detoxification at least in the presence of PDTC. Thus, we believe that PDTC-promotes zinc storage through zinc-binding proteins such as Sod1 (Fig. 3B), as well as vacuolar detoxification, thereby disturbing intracellular metal ion balance causing cross-activation of the iron regulon (Fig. 5).

In higher eukaryotes, PDTC is a known inhibitor of NFκB activation (Schreck et al., 1992). Moreover, it blocks cleavage of the eukaryotic translation initiation factor eIF4G

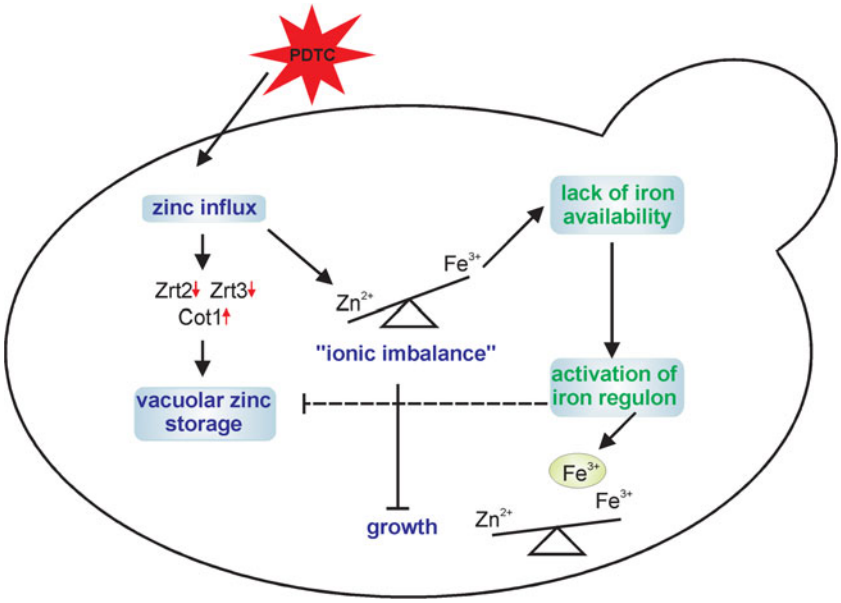

FIG. 6. The ionic imbalance model. PDTC mediates intracellular zinc accumulation, leading to zinc detoxification by vacuolar sequestration, thereby causing a decrease in iron availability. Hence, the iron-dependent transcription factor Aft1 activates the iron regulon and stimulates cellular remodeling as under iron scarcity. Consequently, PDTC might link intracellular disturbance of iron and zinc homeostasis to other cellular processes, including vacuolar and vesicular transport or even pH regulation.

in rhinovirus-infected HeLa cells (Gaudernak et al., 2002). Moreover, PDTC prevents protein degradation by inhibiting a E3 ubiquitin ligase (Hayakawa et al., 2003) or the proteasome (Kim et al., 2004) in a zinc-dependent manner. Hence, it will be interesting for future studies to test whether PDTC can affect related yeast transcription factors such as Rim101, a functional homologue of NFκB implicated in pH regulation, especially because several deletion strains defective in alkaline pH regulation are also PDTC sensitive (Fig. 4; Table 2 Supplementary Data).

Taken together, this work demonstrates the importance of yeast as a model system for performing chemical genetics approaches at the genome-wide scale and its high potential for drug target identification. By combining transcriptional profiling datasets and genome-wide phenotypic screening, it is possible to identify complex and highly dynamic regulatory networks to disclose various biological processes involved in the response to a single drug.

Conclusion

In this study, we successfully exploit genome-wide screening tools and microarray profiling techniques in the eukaryotic model organism *Saccharomyces cerevisiae* to identify genes, processes, and signaling pathways involved in the response to the antiviral drug PDTC. The transcriptional changes upon PDTC treatment involve more than 200 genes, including general stress response genes and other specific adaptations such as an intense crosstalk in metal ion homeostasis. The general stress response genes are involved in growth-related processes, RNA metabolism, and repression of ribosomal protein genes. Interestingly, the specific response comprises of many genes involved in metal ion homeostasis, particularly genes of the iron regulon requiring Aft1-dependent activation and cellular remodeling as necessary during iron limitation. Furthermore, transcriptional regulation of cellular zinc transporters and fluorescent visualization of intracellular zinc accumulation hint a PDTC-induced zinc influx and vacuolar zinc sequestration.

By systematically screening of the yeast gene deletion collection, we identify about 140 genes that are essential for PDTC tolerance. The main functional categories comprise vacuolar acidification and vacuolar transport, protein modifications, mitochondrial organization, and translation. Many of these genes have previously been identified as non-transporter multidrug resistance genes, especially under excess zinc and alkaline pH stress conditions. By combining microarray datasets with phenotypic screening results, we suggest PDTC-induced increase in the intracellular zinc content leading to vacuolar zinc storage accompanied by iron-limitation and full activation of the iron regulon.

Acknowledgments

This work was supported by WWTF Grant "Molecular Mechanisms of Antivirals" (Vienna Science and Technology Fund) to J.S. and K.K., and in part by the FP7-Integrated Project *UNICELLSYS* to K.K. We thank Ralf Egner for providing the yeast strain lacking the Pdr5 and Pdr12 ABC transporters.

Author Disclosure Statement

No competing financial interests exist.

References

Bharucha, N., and Kumar, A. (2007). Yeast genomics and drug target identification. Comb Chem High Throughput Screen 10, 618–634.

Borrello, S., and Demple, B. (1997). NF kappa B-independent transcriptional induction of the human manganous superoxide dismutase gene. Arch Biochem Biophys 348, 289–294.

De Freitas, J.M., Liba, A., Meneghini, R., Valentine, J.S., and Gralla, E.B. (2000). Yeast lacking Cu-Zn superoxide dismutase show altered iron homeostasis. Role of oxidative stress in iron metabolism. J Biol Chem 275, 11645–11649.

Dubacq, C., Chevalier, A., Courbeyrette, R., Petat, C., Gidrol, X., and Mann, C. (2006). Role of the iron mobilization and oxidative stress regulons in the genomic response of yeast to hydroxyurea. Mol Genet Genomics 275, 114–124.

Eide, D.J. (2009). Homeostatic and adaptive responses to zinc deficiency in *Saccharomyces cerevisiae*. J Biol Chem 284, 18565–18569.

Eide, D.J., Clark, S., Nair, T.M., Gehl, M., Gribskov, M., Guerinot, M.L., et al. (2005). Characterization of the yeast ionome: a genome-wide analysis of nutrient mineral and trace element homeostasis in *Saccharomyces cerevisiae*. Genome Biol 6, R77.

Emerson, L.R., Nau, M.E., Martin, R.K., Kyle, D.E., Vahey, M., and Wirth, D.F. (2002). Relationship between chloroquine toxicity and iron acquisition in *Saccharomyces cerevisiae*. Antimicrob Agents Chemother 46, 787–796.

Ericson, E., Gebbia, M., Heisler, L.E., Wildenhain, J., Tyers, M., Giaever, G., et al. (2008). Off-target effects of psychoactive drugs revealed by genome-wide assays in yeast. PLoS Genet 4, e1000151.

Erl, W., Weber, C., and Hansson, G.K. (2000). Pyrrolidine dithiocarbamate-induced apoptosis depends on cell type, density, and the presence of Cu(2+) and Zn(2+). Am J Physiol Cell Physiol 278, C1116–C1125.

Foury, F. (1997). Human genetic diseases: a cross-talk between man and yeast. Gene 195, 1–10.

Gasch, A.P., Spellman, P.T., Kao, C.M., Carmel-Harel, O., Eisen, M.B., Storz, G., et al. (2000). Genomic expression programs in the response of yeast cells to environmental changes. Mol Biol Cell 11, 4241–4257.

Gaudernak, E., Seipelt, J., Triendl, A., Grassauer, A., and Kuechler, E. (2002). Antiviral effects of pyrrolidine dithiocarbamate on human rhinoviruses. J Virol 76, 6004–6015.

Giaever, G. (2003). A chemical genomics approach to understanding drug action. Trends Pharmacol Sci 24, 444–446.

Gitan, R.S., and Eide, D.J. (2000). Zinc-regulated ubiquitin conjugation signals endocytosis of the yeast Zrt1 zinc transporter. Biochem J 346(Pt 2), 329–336.

Gross, C., Kelleher, M., Iyer, V.R., Brown, P.O., and Winge, D.R. (2000). Identification of the copper regulon in *Saccharomyces cerevisiae* by DNA microarrays. J Biol Chem 275, 32310–32316.

Hartsfield, C.L., Alam, J., and Choi, A.M. (1998). Transcriptional regulation of the heme oxygenase 1 gene by pyrrolidine dithiocarbamate. FASEB J 12, 1675–1682.

Haurie, V., Boucherie, H., and Sagliocco, F. (2003). The Snf1 protein kinase controls the induction of genes of the iron uptake pathway at the diauxic shift in *Saccharomyces cerevisiae*. J Biol Chem 278, 45391–45396.

Hausmann, A., Samans, B., Lill, R., and Mühlenhoff, U. (2008). Cellular and mitochondrial remodeling upon defects in iron–sulfur protein biogenesis. J Biol Chem 283, 8318–8330.

Hayakawa, M., Miyashita, H., Sakamoto, I., Kitagawa, M., Tanaka, H., Yasuda, H., et al. (2003). Evidence that reactive oxygen species do not mediate NF-kappaB activation. EMBO J 22, 3356–3366.

Hillenmeyer, M.E., Fung, E., Wildenhain, J., Pierce, S.E., Hoon, S., Lee, W., et al. (2008). The chemical genomic portrait of yeast: uncovering a phenotype for all genes. Science 320, 362–365.

Hughes, T.R., Marton, M.J., Jones, A.R., Roberts, C.J., Stoughton, R., Armour, C.D., et al. (2000). Functional discovery via a compendium of expression profiles. Cell 102, 109–126.

Jin, Y.H., Dunlap, P.E., McBride, S.J., Al-Refai, H., Bushel, P.R., and Freedman, J.H. (2008). Global transcriptome and deletome profiles of yeast exposed to transition metals. PLoS Genet 4, e1000053.

Kaiser, C., Michaelis, S., and Mitchell, A.P. (1994). *Methods in Yeast Genetics. A Laboratory Course Manual.* Cold Spring Harbor, NY: Cold Spring Harbor Laboratory Press.

Kaplan, C.D., and Kaplan, J. (2009). Iron acquisition and transcriptional regulation. Chem Rev 109, 4536–4552.

Kawahata, M., Masaki, K., Fujii, T., and Iefuji, H. (2006). Yeast genes involved in response to lactic acid and acetic acid: acidic conditions caused by the organic acids in *Saccharomyces cerevisiae* cultures induce expression of intracellular metal metabolism genes regulated by Aft1p. FEMS Yeast Res 6, 924–936.

Kim, I., Kim, C.H., Kim, J.H., Lee, J., Choi, J.J., Chen, Z.A., Lee, M.G., et al. (2004). Pyrrolidine dithiocarbamate and zinc inhibit proteasome-dependent proteolysis. Exp Cell Res 298, 229–238.

Kimura, A., Ohashi, K., and Naganuma, A. (2007). Cisplatin upregulates *Saccharomyces cerevisiae* genes involved in iron homeostasis through activation of the iron insufficiency-responsive transcription factor Aft1. J Cell Physiol 210, 378–384.

Krenn, B.M., Holzer, B., Gaudernak, E., Triendl, A., van Kuppeveld, F.J., Seipelt, J. (2005). Inhibition of polyprotein processing and RNA replication of human rhinovirus by pyrrolidine dithiocarbamate involves metal ions. J Virol 79, 13892–13899.

Kumanovics, A., Chen, O.S., Li, L., Bagley, D., Adkins, E.M. Lin, H., et al. (2008). Identification of *FRA1* and *FRA2* as genes involved in regulating the yeast iron regulon in response to decreased mitochondrial iron-sulfur cluster synthesis. J Biol Chem 283, 10276–10286.

Lanke, K., Krenn, B.M., Melchers, W.J., Seipelt, J., and van Kuppeveld, F.J. (2007). PDTC inhibits picornavirus polyprotein processing and RNA replication by transporting zinc ions into cells. J Gen Virol 88, 1206–1217.

Li, L., and Kaplan, J. (1998). Defects in the yeast high affinity iron transport system result in increased metal sensitivity because of the increased expression of transporters with a broad transition metal specificity. J Biol Chem 273, 22181–22187.

MacDiarmid, C.W., Milanick, M.A., and Eide, D.J. (2002). Biochemical properties of vacuolar zinc transport systems of *Saccharomyces cerevisiae*. J Biol Chem 277, 39187–39194.

Mamnun, Y.M., Schüller, C., and Kuchler, K. (2004). Expression regulation of the yeast *PDR5* ATP-binding cassette (ABC) transporter suggests a role in cellular detoxification during the exponential growth phase. FEBS Lett 559, 111–117.

Morais, C., Pat, B., Gobe, G., Johnson, D.W., and Healy, H. (2006). Pyrrolidine dithiocarbamate exerts anti-proliferative and pro-apoptotic effects in renal cell carcinoma cell lines. Nephrol Dial Transplant 21, 3377–3388.

Moreno, S., Klar, A., and Nurse, P. (1991). Molecular genetic analysis of fission yeast *Schizosaccharomyces pombe*. Methods Enzymol 194, 795–823.

Outten, C.E., Falk, R.L., and Culotta, V.C. (2005). Cellular factors required for protection from hyperoxia toxicity in *Saccharomyces cerevisiae*. Biochem J 388, 93–101.

Pagani, M.A., Casamayor, A., Serrano, R., Atrian, S., and Arino, J. (2007). Disruption of iron homeostasis in *Saccharomyces cerevisiae* by high zinc levels: a genome-wide study. Mol Microbiol 65, 521–537.

Parsons, A.B., Brost, R.L., Ding, H., Li, Z., Zhang, C., Sheikh, B., et al. (2004). Integration of chemical-genetic and genetic interaction data links bioactive compounds to cellular target pathways. Nat Biotechnol 22, 62–69.

Parsons, A.B., Lopez, A., Givoni, I.E., Williams, D.E., Gray, C.A., Porter, J., et al. (2006). Exploring the mode-of-action of bioactive compounds by chemical-genetic profiling in yeast. Cell 126, 611–625.

Pfaller, M.A., and Diekema, D.J. (2004). Rare and emerging opportunistic fungal pathogens: concern for resistance beyond *Candida albicans* and *Aspergillus fumigatus*. J Clin Microbiol 42, 4419–4431.

Raju, B., Murphy, E., Levy, L.A., Hall, R.D., and London, R.E. (1989). A fluorescent indicator for measuring cytosolic free magnesium. Am J Physiol 256, C540–C548.

Rutherford, J.C., and Bird, A.J. (2004). Metal-responsive transcription factors that regulate iron, zinc, and copper homeostasis in eukaryotic cells. Eukaryot Cell 3, 1–13.

Saeed, A.I., Sharov, V., White, J., Li, J., Liang, W., Bhagabati, N., et al. (2003). TM4: a free, open-source system for microarray data management and analysis. Biotechniques 34, 374–378.

Saeed, A.I., Bhagabati, N.K., Braisted, J.C., Liang, W., Sharov, V., Howe, E.A., et al. (2006). TM4 microarray software suite. Methods Enzymol 411, 134–193.

Sambrook, J., Fritsch, E., and Maniatis, T. (2001). *Molecular Cloning: A Laboratory Manual.* 3rd ed. New York: Cold Spring Harbor Press.

Santos, P.M., Simoes, T., and Sa-Correia, I. (2009). Insights into yeast adaptive response to the agricultural fungicide mancozeb: a toxicoproteomics approach. Proteomics 9, 657–670.

Santos, R., Dancis, A., Eide, D., Camadro, J.M., and Lesuisse, E. (2003). Zinc suppresses the iron-accumulation phenotype of *Saccharomyces cerevisiae* lacking the yeast frataxin homologue (Yfh1). Biochem J 375, 247–254.

Schreck, R., Meier, B., Mannel, D.N., Droge, W., and Baeuerle, P.A. (1992). Dithiocarbamates as potent inhibitors of nuclear factor kappa B activation in intact cells. J Exp Med 175, 1181–1194.

Serrano, R., Ruiz, A., Bernal, D., Chambers, J.R., and Arino, J. (2002). The transcriptional response to alkaline pH in *Saccharomyces cerevisiae*: evidence for calcium-mediated signalling. Mol Microbiol 46, 1319–1333.

Serrano, R., Bernal, D., Simon, E., and Arino, J. (2004). Copper and iron are the limiting factors for growth of the yeast *Saccharomyces cerevisiae* in an alkaline environment. J Biol Chem 279, 19698–19704.

Simons, T.J. (1993). Measurement of free Zn2 + ion concentration with the fluorescent probe mag-fura-2 (furaptra). J Biochem Biophys Methods 27, 25–37.

Smyth, G.K. (2004). Linear models and empirical bayes methods for assessing differential expression in microarray experiments. Stat Appl Genet Mol Biol 3, Article3.

Stadler, J.A., and Schweyen, R.J. (2002). The yeast iron regulon is induced upon cobalt stress and crucial for cobalt tolerance. J Biol Chem 277, 39649–39654.

Stockwell, B.R. (2000). Chemical genetics: ligand-based discovery of gene function. Nat Rev Genet 1, 116–125.

Tarhan, C., Pekmez, M., Karaer, S., Arda, N., and Sarikaya, A.T. (2007). The effect of superoxide dismutase deficiency on zinc

toxicity in *Schizosaccharomyces pombe*. J Basic Microbiol 47, 506–512.

Teixeira, M.C., Monteiro, P., Jain, P., Tenreiro, S., Fernandes, A.R., Mira, N.P., et al. (2006). The YEASTRACT database: a tool for the analysis of transcription regulatory associations in *Saccharomyces cerevisiae*. Nucleic Acids Res 34, D446–D451.

Tucker, C.L., and Fields, S. (2004). Quantitative genome-wide analysis of yeast deletion strain sensitivities to oxidative and chemical stress. Comp Funct Genomics 5, 216–224.

Uchide, N., Ohyama, K., Bessho, T., Yuan, B., and Yamakawa, T. (2002). Effect of antioxidants on apoptosis induced by influenza virus infection: inhibition of viral gene replication and transcription with pyrrolidine dithiocarbamate. Antiviral Res 56, 207–217.

Wettenhall, J.M., and Smyth, G.K. (2004). limmaGUI: a graphical user interface for linear modeling of microarray data. Bioinformatics 20, 3705–3706.

Wu, W.S., Li, W.H., and Chen, B.S. (2008). Reconstructing a network of stress-response regulators via dynamic system modeling of gene regulation. Gene Regul Syst Biol 2, 53–62.

Yamaguchi-Iwai, Y., Dancis, A., and Klausner, R.D. (1995). *AFT1*: a mediator of iron regulated transcriptional control in *Saccharomyces cerevisiae*. EMBO J 14, 1231–1239.

Yamaguchi-Iwai, Y., Ueta, R., Fukunaka, A., and Sasaki, R. (2002). Subcellular localization of Aft1 transcription factor responds to iron status in *Saccharomyces cerevisiae*. J Biol Chem 277, 18914–18918.

Yun, C.W., Ferea, T., Rashford, J., Ardon, O., Brown, P.O., Botstein, D., et al. (2000). Desferrioxamine-mediated iron uptake in *Saccharomyces cerevisiae*. Evidence for two pathways of iron uptake. J Biol Chem 275, 10709–10715.

Address correspondence to:
Karl Kuchler
Medical University Vienna
Max F. Perutz Laboratories
Campus Vienna Biocenter
A-1030 Vienna, Dr. Bohr-Gasse 9/2, Austria

E-mail: karl.kuchler@meduniwien.ac.at